Differentiation of Mouse induced Pluripotent Stem Cells into Alveolar Epithelial Cells *In Vitro* for Use *In Vivo*

Qiliang Zhou1, Xulu Ye1, Ruowen Sun2, Yoshifumi Matsumoto1, Masato Moriyama1, Yoshiya Asano3, Yoichi Ajioka4, and Yasuo Saijo1*

1Department of Medical Oncology, Niigata University Graduate School of Medical and Dental Sciences

2Department of Pediatric Hematology, Shengjing Hospital of China Medical University, Shenyang, China

3Department of Neuroanatomy, Cell Biology and Histology, Hirosaki University Graduate School of Medicine

4Division of Molecular and Diagnostic Pathology, Niigata University Graduate School of Medical and Dental Sciences

Running Title: Lung re-construction by differentiated iPS Cells

*To whom correspondence should be addressed:

Department of Medical Oncology, Niigata University Graduate School of Medical and Dental Sciences, 1-757 Asahimachi-dori Chuoh-ku, Niigata 951-8510, Japan

TEL: +81-25-368-9003; FAX: +81-25-368-9005; E-mail: yasosj@med.niigata-u.ac.jp

ABSTRACT

Alveolar epithelial cells (AECs) differentiated from induced pluripotent stem cells (iPSCs) represent new opportunities in lung tissue engineering and cell therapy. In this study, we modified a two-step protocol for embryonic stem cells that resulted in a yield of ~9% SPC^+ alveolar epithelial type II (AEC II) cells from mouse iPSCs in a 12-day period. The differentiated iPSCs showed morphological characteristics similar to those of AEC II cells. When differentiated iPSCs were seeded and cultured in a mouse decellularized lung scaffold, the cells re-formed an alveolar structure and expressed SPC or T1α protein, markers of AEC II or AEC I cells, respectively. Finally, the differentiated iPSCs were instilled intratracheally into a bleomycin (BLM)-induced mouse acute lung injury model. The transplanted cells integrated into the lung alveolar structure and expressed SPC and T1α. Significantly reduced lung inflammation and decreased collagen deposition were observed following differentiated iPSC transplantation. In conclusion, we report a simple and rapid protocol for *in vitro* differentiation of mouse iPSCs into AECs. Differentiated iPSCs show potential for regenerating three-dimensional alveolar lung structure and can be used to abrogate lung injury.

INTRODUCTION

In the advanced stage of acute and chronic lung diseases, such as acute lung injuries, idiopathic pulmonary fibrosis (IPF), and chronic obstructive lung disease (COPD), present medications can only stabilize the disease conditions or delay disease progression. Although lung transplantation is the only definitive option for these advanced-stage lung diseases, donor organ shortage is a major problem.

Tissue engineering regenerative medicine is a new multidisciplinary field for exchanging impaired cells or tissues with new functional cells or tissues. The first step in regenerative medicine for end-stage lung diseases is generation of alveolar epithelium containing two cell types: alveolar epithelial type I and type II cells (AEC I and II). AEC I cells are large, flattened cells comprising 95% of the alveolar lining area and are responsible for gas exchange, whereas AEC II cells are cuboidal cells, more abundant but smaller than AEC I cells, which comprise 5% of the alveolar lining area [1,2]. AEC I cells are terminally differentiated, unable to replicate, and are susceptible to environmental toxicants and pathogens. In the event of lung damage, although AEC II cells have been shown to undergo proliferation and/or differentiation to AEC I cells to repair the damaged alveolar epithelium, this repair process often causes inappropriate reconstruction of lung structures [1,3,4].

Embryonic stem cells (ESCs) are self-renewing pluripotent cells that can differentiate into alveolar epithelial cells *in vitro* [5-16]. The problems of immune rejection and ethical issues restrict clinical application of ESCs. Induced pluripotent stem cells (iPSCs), which are derived from differentiated somatic cells by introduction of several defined transcription factors, display self-renewal properties and pluripotency similar to ESCs [17,18]. Additionally, they have the potential to overcome the abovementioned limitations. Recently, several studies have reported *in vitro* differentiation to AEC II-like cells from iPSCs [19,20].

In the present study, we differentiated mouse iPSCs into AECs *in vitro* and investigated the regenerative and therapeutic potential of those differentiated iPSCs in mouse models. We used a previously reported two-step protocol to differentiate iPSCs into AECs. Although most ESC differentiation protocols have used the conventional embryoid body

(EB) method [9], we achieved iPSC differentiation using a dissociated low-density seeding method that is considered more rapid and effective [10]. We tested six medium combinations to identify the most efficient protocol and successfully differentiated mouse iPSCs into AEC-like cells. The regenerative potential was demonstrated through seeding of the differentiated iPSCs into decellularized mouse lung scaffolds. Their therapeutic potential was demonstrated in a bleomycin-induced mouse acute lung injury model.

MATERIALS AND METHODS

Cell Line and Cell Culture

A mouse iPS cell line (iPS-MEF-Ng-492B-4) obtained from the RIKEN Cell Bank (Tsukuba, Japan) was maintained on 1×10^4 cells/cm^2 mitomycin-C (Sigma-Aldrich, St Louis, MO, USA)-inactivated mouse SNL76/7 cells (ECACC; #EC07032801) as a feeder layer on 0.1% gelatin-coated tissue culture dishes in iPS medium containing high-glucose Dulbecco's modified Eagle's medium (DMEM; Gibco, Carlsbad, CA, USA) supplemented with 15% ES cell fetal bovine serum (FBS; Gibco), 0.1 mM nonessential amino acids (Gibco), 0.1 mM 2-mercaptoethanol (Gibco), 1000 U/ml mLIF (Chemicon, Temecula, CA, USA), 50 U/mL penicillin, and 50 mg/mL streptomycin (Gibco).

The murine type II pneumocyte cell line MLE12 was obtained from the American Type Culture Collection (ATCC, Manassas, VA, USA; #CRL-2110) and was cultured in medium containing 50% DMEM (Gibco) and 50% Ham's F12 medium (Gibco) supplemented with 10 nM hydrocortisone (Sigma-Aldrich), 10 nM β-estradiol (Sigma-Aldrich), 10 nM HEPES (Sigma-Aldrich), 2 nM L-glutamine (Gibco), 1% ITS

(Gibco), 2% FBS (Gibco), 50 U/mL penicillin, and 50 mg/mL streptomycin (Gibco).

Mouse iPSC Differentiation

Mouse iPSCs were induced to differentiate into AECII-like cells using the dissociated seeding method for murine ESCs described previously, with slight modifications [10]. As shown in Figure 1A, at first, mouse iPSCs were trypsinized, centrifuged, resuspended in iPS medium, and plated at a lower density (1×10^3cells/cm^2) on 0.1% gelatin-coated tissue culture dishes for 24 h. Next, the iPS medium was changed to basic differentiation medium (Basic DM) supplemented with 20 ng/ml Activin A (R&D Systems, Minneapolis, MN, USA) and 10 ng/ml Wnt3a (R&D Systems), and then incubated for 6 days (D1–D7). Basic DM contains 75% IMDM (Gibco) and 25% Ham's F12 medium (Gibco) supplemented with 0.5× of both N2 and B27 (without retinoic acid) supplements (Gibco), 50 U/ml penicillin, 50 mg/ml streptomycin, 2 mM glutamine (Gibco), 0.5 mM ascorbic acid (Sigma-Aldrich), 4.5×10^{-4} M 1-thioglycerol (Sigma-Aldrich), and 0.05% bovine serum albumin (BSA; Sigma-Aldrich). Next, the differentiation medium was changed to fresh Basic DM or small-airway basal medium (SABM) (Lonza, Walkersville, MD, USA) supplemented with 50 ng/ml FGF2 (Sigma-Aldrich) and 50 μg/ml heparin sulfate salt (Sigma-Aldrich), followed by incubation for a further 5 days.

Immunofluorescence

Mouse lung tissues were frozen or fixed with 4% paraformaldehyde and embedded in paraffin. Paraffin-embedded sections were deparaffinized, and antigen retrieval was subsequently performed by autoclaving the tissue sections in antigen retrieval solution

(Nichirei, Tokyo, Japan; #415211) at 120°C for 10 min. Sections were blocked with Protein Block Serum-Free (Dako; #X0909) for 20 min at room temperature, and then were incubated with primary antibody at 4°C overnight. Sections were incubated with secondary antibody for 1 h at room temperature. Sections were stained with DAPI for nuclear counterstaining and mounted with VECTASHIELD Mounting Medium (Vector Laboratories, Burlingame, CA, USA; #H-1500). All fluorescent photographs were acquired using a Nikon C1si Confocal Microscope with the Nikon EZ-C1 software.

To quantify SPC-positive cells, five images (400× magnification) were randomly selected in at least two slides per mouse lung (5 mice/group) to be counted visually. For staining of iPSCs, cells were seeded in 0.1% gelatin-coated four-well tissue culture Permanox chamber slides (Thermo Fisher Scientific, Waltham, MA, USA). The cells on days 7 and 12 of the differentiation protocol were fixed in 4% paraformaldehyde for 15 min and permeabilized for 10 min in 0.2% Triton X-100/phosphate-buffered saline (PBS) on ice. Next, the cells were blocked and stained as described above.

Primary antibodies were goat SPC (1:500; Santa Cruz Biotechnology, Santa Cruz, CA, USA; #SC-7706), goat T1α (1:100; Santa Cruz Biotechnology; #SC-23564), mouse SSEA1 (1:100; STEMGENT, San Diego, CA, USA; #09-0005), rabbit OCT3/4 (1:100; STEMGENT; #09-0023), goat Sox17 (1:100; Santa Cruz Biotechnology; #SC-17355), goat Foxa2 (1:100; Santa Cruz Biotechnology; #SC-6554). The appropriate goat, rabbit, and mouse IgG or IgM was used as the isotype control. Secondary antibodies were donkey anti-goat IgG-Alexa Fluor 488 (1:200; Invitrogen, Carlsbad, CA, USA; #A11055), goat anti-mouse IgM–cy3 (1:200; Biorbyt, San Francisco, CA, USA; #orb14378), donkey anti-goat IgG-Alexa Fluor 594 (1:200; Invitrogen; #A11058), and goat anti-rabbit IgG-Alexa Fluor 594 (1:200; Invitrogen;

#A11012).

Real-time Reverse Transcription-Polymerase Chain Reaction (RT-PCR)

Total RNA of iPSCs was extracted using an RNeasy kit (Qiagen, Valencia, CA, USA), and reverse transcriptase reactions were performed using aliquots of 2 μg of total RNA using the High-capacity cDNA Reverse Transcription kit (Applied Biosystems, Carlsbad, CA) according to the manufacturer's protocol. Quantitative real-time PCR was performed in triplicate using the TaqMan Universal PCR Master Mix and TaqMan Gene Expression Assay (Applied Biosystems) in an ABI 7900HT sequence detection system (Applied Biosystems). The conditions for real-time PCR were 50°C (2 min), 95°C (10 min), followed by 50 cycles of 95°C (15 s) and 60°C (1 min). The TaqMan Gene Expression Assay IDs of detected genes were Mm01976556_s1 (Foxa2), Mm00488363_m1 (Sox17), Mm00499170_m1 (SPA), Mm00455681_m1 (SPB), Mm00488144_m1 (SPC), Mm00486060_m1 (SPD), Mm00442046_m1 (CCSP), and Mm99999915_g1 (GAPDH). GAPDH was used as an endogenous control gene, and the average value of the undifferentiated iPSCs was used as the calibrator. Calculations were performed using the comparative C_T method.

Flow Cytometry

Flow cytometry was performed for quantifying the SPC-positive cells after differentiation. Briefly, cells were dissociated into a single-cell suspension in PBS containing 1 mM EDTA and 3% FBS (flow cytometry buffer), fixed and permeabilized for intracellular antigen (SPC) with Intraprep permeabilization reagent (Beckman Coulter, Fullerton, CA, USA; #A07802) according to the manufacturer's protocol. The

cells were stained for 30 min on ice with goat anti-mouse SPC (Santa Cruz Biotechnology; #sc-7706), followed by phycoerythrin (PE)-conjugated donkey anti-goat IgG. Goat IgG was used as an isotype control. Finally, cells were analyzed by flow cytometry (Cell Lab Quanta SC; Beckman Coulter).

Transmission Electron Microscopy (TEM)

The murine type II pneumocyte cell line MLE12 and mouse iPSCs were washed with 1× PBS and centrifuged for 5 min at 300 × g. The cell pellets were fixed with 2% paraformaldehyde/1% glutaraldehyde in 0.1 M PBS at 4°C overnight, washed with 1× PBS, and post-fixed with 1% OsO4 in 0.1 M PBS for 30 min at room temperature. The cell pellets were then washed three times in PBS and dehydrated in graded ethanol solutions. The cells were moved to a 500-µl embedding tube and treated with propylene oxide for 15 min after centrifugation. The cell pellets were infiltrated at 1:1 propylene oxide/Epon at room temperature overnight. The following day, the samples were centrifuged for 3 min at 800 × g, infiltrated at 1:4 propylene oxide/Epon at room temperature for 1 h, centrifuged for 3 min at 800 × g again, exposed to 100% Epon for 1 h at room temperature, and finally incubated at 60°C for 48 h. Ultrathin sections (50 nm) were cut and collected on sheet mesh, stained with uranyl acetate and lead citrate. The stained sections were examined and photographed in a JEM-1230 TEM (JEOL, Tokyo, Japan) at 80-kV voltage.

Lung Decellularization and Recellularization

Mouse lung decellularization and recellularization were performed according to methods reported recently [15,21]. Briefly, harvested heart-lung blocs were

decellularized by injection of 0.1% sodium dodecyl sulfate (Sigma-Aldrich) and 1% Triton X-100 (Sigma-Aldrich) through both the right ventricle and trachea. Cells in complete medium were mixed with 2% low-melting-point agarose at 37°C to generate a suspension. One milliliter of cell suspension (2×10^6 cells/ml) in 2% low-melting-point agarose was injected intratracheally into the decellularized lung. Lungs were then incubated for 5 min on ice until the agarose hardened and were sectioned into approximately 2-mm thick slices using a sterile surgical blade (Fig.3A). The lung sections were cultured in small airway epithelial cell growth medium (Lonza) for 12 days, and then fixed with 10% formaldehyde and embedded in paraffin.

Intratracheal Transplantation of Differentiated iPSCs into Bleomycin (BLM)-injured Mouse Lungs

All mouse experiments were approved by the Institutional Animal Care and Use Committee of Niigata University. Pathogen-free female mice in a C57BL/6N genetic background (8-week-old, 18 to 20-g body weight; Charles River Laboratories, Yokohama, Japan) were anesthetized by intraperitoneal injection of 0.5 mg/g Avertin (Sigma-Aldrich), and then were administered either 4 units/kg BLM (Sigma-Aldrich) or sterile normal saline by intratracheal instillation via oropharynx intubation using a liquid aerosol device and a small animal laryngoscope (Penn-Century, Wyndmoor, PA). Oropharynx intubation allows subsequent noninvasive cell transplantation after BLM treatment [11]. The next day, the BLM-injured mice were transplanted with fibroblasts, undifferentiated iPSCs, or differentiated iPSCs (5×10^5 cells/mouse). The mice were euthanized on day 13, and lungs were harvested. Transplanted cells were identified by labeling with the PKH26 Red Fluorescent Cell Linker Mini Kit (Sigma-Aldrich)

according to the manufacturer's protocol.

Bronchoalveolar lavage (BAL) and ELISA

After euthanasia on day 12, the trachea was cannulated with a 24-gauge catheter. The airway was lavaged with four consecutive washes of 0.5 ml sterile PBS. BAL fluid was centrifuged at 1,200 rpm for 15 min at 4°C, and the supernatants were stored at -80°C until use. Cell pellets were resuspended in 1 ml ice-cold RPMI-1640 media and centrifuged onto glass slides at 600 rpm for 10 min in a Shandon Cytospin 4 cytocentrifuge (Thermo Scientific, Waltham, USA). Cells were stained using the Diff-Quik stain set (Sysmek, Kobe, Japan). TNF-α and IL-6 concentrations in BAL fluid were measured using solid phase sandwich ELISA kits (Invitrogen; #KMC3011 for TNF-α, #KMC0061 for IL-6) according to the manufacturer's protocol.

Wet/Dry Weight Ratio

The wet/dry weight ratio of the lung was measured to quantitatively evaluate the degree of pulmonary inflammation induced by BLM treatment according to a method described previously [22,23]. The wet weight of lungs was measured immediately after sacrifice. The lungs were then placed with a desiccant in an oven at 60°C for 4 days and reweighed to determine the dry weight.

Measurement of Lung Collagen

Sirius red/fast green staining was performed to evaluate collagen deposition in lung tissues. Briefly, paraffin sections of lung tissue were deparaffinized, hydrated, and incubated in 0.1% Fast Green (Wako, Tokyo, Japan; #069-00032) for 1 h at room

temperature, washed in 0.5% acetic acid (Wako) for 5 min and rinsed in tap water. Sections were then incubated in 0.1% Sirius red (Sigma-Aldrich; #365548) in saturated aqueous picric acid (Wako) for 1 h at room temperature and washed with 0.5% acetic acid for 5 min twice. After rinsing with tap water, sections were rapidly dehydrated and mounted in xylene. Collagen deposition was also assessed using a Hydroxyproline Assay Kit (BioVision, Milpitas, CA, USA; #K555-100) according to the manufacturer's protocol. Briefly, 50 mg of homogenized lung sample were incubated in 1 ml of 6 N HCL at 110°C overnight. The hydrolyzed samples were neutralized with 1 ml of 6 N NaOH, filtered through a 0.1-mm filter, and then incubated with 100-µl Chloramine T reagent for 5 min at room temperature. One hundred microliters of the DMAB reagent were then added and incubated for 90 min at 60°C. The absorbance was measured at 570 nm, and the hydroxyproline content was calculated against a standard curve.

Statistical Analysis

The data are presented as means ± standard deviation. One-way analysis of variance (ANOVA) and Tukey-Kramer tests were used to assess the significance of differences. A *P* value less than 0.05 was deemed to indicate statistical significance.

RESULTS

Decision of Differentiation Medium through mRNA Expression Levels of Endoderm and Lung Epithelium Markers

We maintained mouse iPSCs and monitored the undifferentiated status of iPSCs until passage 35. iPSC pluripotency was maintained according to alkaline phosphatase (AP) staining and immunostaining for the mouse pluripotency markers SSEA1, Nanog, and

OCT4. iPSCs were positive for all of these pluripotency markers (Fig. S1). Mouse iPSCs from passages 10 to 30 were used in the present study.

Because the GFP gene was knocked-in the mouse iPS cell line under the Nanog promoter, the undifferentiated iPSCs could be surveyed by detecting GFP expression throughout the differentiation procedure [24]. Around 4% GFP^+ cells remained at the end of differentiation stage 1 (day 7), whereas no GFP^+ cells were observed at the end of differentiation stage 2 (day 12) (data not shown). The definitive endoderm markers Sox17 and Foxa2 were expressed on day 7 (Fig. S2A). The BSA-free condition further enhanced the expression levels of Sox17 and Foxa2 (55.8±6.4-fold *vs.* 37.9±3.5-fold, respectively; 326.4±33-fold *vs.* 201.5±45.5-fold, respectively; $P<0.05$) (Fig. S2B). The mRNA expression levels of the lung epithelial markers surfactant protein A (SPA), surfactant protein B (SPB), surfactant protein C (SPC), surfactant protein D (SPD), Clara cell secretory protein (CCSP), and thyroid transcription factor 1 (TTF-1, also known as Nkx2-1) were markedly increased compared with undifferentiated iPSCs (Fig. 1B) at the end of stage 2 differentiation (day 12). Small airway basic medium (SABM) enhanced the mRNA expression of SPA, SPC, and SPD, but it decreased that of TTF1 compared with Basic DM when applied during stage 2 differentiation (*$P<0.05$). The presence of BSA in SABM decreased the mRNA expression of SPA and SPC (#$P<0.01$) compared with its absence. Because SPC is a specific marker of alveolar type 2 cells, we used the medium combination that resulted in the greatest SPC mRNA expression after completion of two-step differentiation. The mRNA expression of SPA was increased by 116.3±26.5-fold, SPB by 28.8±12.6-fold, SPC by 8.3±2.4-fold, SPD by 9.1±0.6-fold, CCSP by 4.8±2.4-fold, and TTF1 by 168.6±88.4 fold in the condition described above. However, the mRNA expression of lung epithelial markers in

differentiated iPSCs was lower than that of positive controls (MLE12 cells and mouse lung tissue) (Figure 1C). Nevertheless, these differentiated iPS cells expressed lung epithelial markers. As shown in Figure 1A, we used Basic DM + Activin A (20 ng/ml) + Wnt3a (10 ng/ml) in stage 1 and SABM+FGF2 (50 ng/ml) in stage 2 as differentiation media in the following experiments.

Evaluation of Differentiated iPSC Phenotypes

SPC protein expression in the cytoplasm of differentiated iPSCs was confirmed by immunofluorescence (Fig. 2A). Additionally, 9.3±3.3% SPC-positive differentiated iPSCs were detected by flow cytometry (Fig. 2B). TEM ultrastructural analysis showed characteristic lamellar bodies and microvilli, organelles specific to alveolar type 2 cells, in differentiated iPSCs on day 12 (Fig. 2C). These data demonstrated that a portion of iPSCs differentiated into AECs, particularly alveolar type 2 cells.

Recellularization of Decellularized Mouse Lung Scaffold with iPSC-Derived AECs

We assessed the regenerative potential of iPSC-derived AECs in a mouse decellularized lung scaffold model that was recently demonstrated to be useful for studying functional recellularization in stem and progenitor cell populations [15, 25]. After 12 days of incubation, iPSC-derived AECs were observed to integrate into the parenchymal regions and form alveolar structures (Fig. 3B). Some of them adopted the morphology of alveolar epithelia; *i.e.*, they developed a rounded or flattened shape (Figs. 3B and 4). However, the undifferentiated iPSCs tended to proliferate in the alveolar space and form masses of cells, which resembled colonies (Figs. 3B and 4). The fibroblasts survived but were integrated into the stroma of the lung. Immunofluorescence staining showed

strong expression of SPC and T1α in tissues of the iPSC-derived AEC group, whereas few SPC- or T1α-positive cells were detected in the undifferentiated iPSC group (Fig.4). No SPC or T1α expression was detected in the fibroblast group (Fig. 4). When SPC-positive cells were quantified in the recellularized mouse lung scaffolds by iPSC-derived AEC, we observed an increased percentage of SPC-positive cells (13.46±5.59%) after 12 days compared to those in *in vitro* differentiation D12 (9.3±3.3%). No further improvement in alveolar morphology structure or lung epithelium marker expression was observed when the culture duration was prolonged to 30 days (data not shown).

Transplantation of Differentiated iPSCs in a Lung Injury Mouse Model

To examine whether transplanted cells could home to and ameliorate lung injury, iPSC-derived AECs, undifferentiated iPSCs, or fibroblasts were delivered intratracheally into a BLM-induced lung injury mouse model. Using PKH26 staining, we succeeded in providing a convenient strategy to track the donor cells after transplantation into the mouse lung. As shown in Figs. 5 and S3, the transplanted cells (red) showed uniform distribution throughout the distal alveoli on day 12 after transplantation.

After BLM treatment, the numbers of SPC-positive and T1α-positive cells were drastically reduced (Figs. 5 and S3). Transplantation of iPSC-derived AECs recovered the numbers of SPC-positive cells (from 6.6±3.1% to 12.1±3.3%, $P<0.05$, Fig S4A) and T1α-positive cells in the BLM-treated lung. Transplantation of undifferentiated iPSCs modestly recovered the numbers of SPC-positive (8.2±2.6%, $P>0.05$, Fig S4A) and T1α-positive cells. No recovery of SPC-positive or T1α-positive cells was observed

after fibroblast transplantation.

In addition, $SPC^+/PKH26^+$ and $T1a^+/PKH26^+$ cells were observed in lung sections only in the iPSC-derived AEC group (Figs. 5 and S3). No $SPC^+/PKH26^+$ or $T1\alpha^+/PKH26^+$ cells were detected in the fibroblast or undifferentiated iPSC groups. Because of the non-uniform composition of the cell population and longer centrifugation time (four × 10 min) needed in our PKH26 staining protocol, the viability of iPSC-derived AECs might be reduced. Thus, the frequency of double-positive cells was stochastic and might be quantified as being lower. We did not quantify double-positive cells in lung sections. Nonetheless, the presence of $SPC^+/PKH26^+$ and $T1\alpha^+/PKH26^+$ cells demonstrated the successful derivation of AECs from iPSCs and their engraftment into the mouse lung. We also evaluated the long-term survival of differentiated iPSCs in BLM-injured mouse lungs. We confirmed the presence of SPC+/PKH26+ and T1α+/PKH26+ cells on day 30 after transplantation, although PKH26 fluorescence became very weak (Fig. S4B).

Transplantation of Differentiated iPSCs Reduces Lung Inflammation and Attenuates Lung Fibrosis in BLM-treated Mice

Twelve days after intratracheal exposure of BLM, the lung tissues were severely damaged as shown by hematoxylin and eosin (HE) staining (Fig. 6A). The lungs presented typical injuries such as disorganized epithelium, extensive inflammatory cell infiltration, interstitial thickening, collapse of the alveolar wall, and obvious cystic air spaces. Increased collagen deposition was observed by Sirius red/Fast green staining and hydroxyproline assay (Fig. 6A and 6C). Wet/dry weight ratios indicated that BLM treatment resulted in a significant increase in edema compared with the saline group (6.1±0.4 *vs.* 4.5±0.2, respectively; $^{**}P<0.01$) (Fig. 6B). Transplantation of

differentiated iPSCs significantly reduced the extent of fibrosis and recovered the lung tissue structure to similar to that of the saline control (Figs. 5, S3, and 6A). A decrease in lung edema was confirmed in the iPSC-derived AEC group compared with the BLM and BLM/fibroblast groups (Fig. 6B; #P<0.01). Transplantation of differentiated iPSCs reduced inflammatory cell infiltration (Fig. 7A) and decreased TNF-α and IL-6 levels in BLM-treated mice to the same levels as in the saline control (Fig. 7B and 7C; † P>0.05). There was no significant decrease in TNF-α and IL-6 production in the undifferentiated iPSC group compared with the BLM and BLM/fibroblasts groups (Fig. 7B and 7C; ▲ P>0.05). Hydroxyproline assay showed that the collagen content was decreased in the lungs of the differentiated iPSC transplantation group compared with the BLM and BLM/fibroblast groups (Fig. 6C; #P<0.01). However, treatment with iPSCs-derived AECs did not result in a return to the basal collagen level (Fig. 6C; *P<0.05). By contrast, there was no significant decrease in lung edema and collagen deposition in the undifferentiated iPSC group compared with the BLM group (Fig. 6B and 6C; ▲P>0.05). Transplantation of fibroblasts did not rescue the lung injuries.

DISCUSSION

In the present study, we report an *in vitro* protocol for direct differentiation of mouse iPSCs into ~9% lung progenitor or epithelial cells in two steps. These differentiated cells express a lung progenitor marker, TTF-1, and a type II alveolar type marker, SP-C. These cells can recellularize a decellularized mouse lung scaffold in three-dimensional culture. Finally, these differentiated cells ameliorated the BLM-induced lung injury and engrafted into the lung.

Stem cell therapy provides a new strategy for repairing severe acute and chronic lung

injuries. Although some studies have demonstrated the therapeutic potential of bone-marrow-derived stem cells in rodent lung injury models [23, 26-28], there is no evidence of a role for these stem cells in populating the lung alveolar epithelium *in vivo* [29-32]. Recent studies have reported efficient and direct derivation of lung alveolar epithelium from murine embryonic stem cells (ESCs) [10,11,14,16] for *in vitro* and *in vivo* applications. However, immune reactions and ethical issues represent barriers to their clinical application.

We modified a protocol for mouse iPSC differentiation into AECs *in vitro* in a 12-day period, and achieved a 9.3±3.3% yield of SPC^+ AEC II-like cells. However, a recent study developed a more efficient differentiation protocol for lung epithelial cells (20). mRNA expression of type II epithelial markers, such as SPA and SPC, was suppressed in the presence of BSA (Fig. 1B), as reported previously [9,33]. SABM enhanced the mRNA expression of SPA, SPC, and SPD but suppressed that of TTF1 compared with Basic DM when used during stage 2 differentiation. A primordial progenitor stage defined by TTF-1 expression is considered essential for formation of lung epithelia differentiated from endodermal cells [15,34,35]. Therefore, use of SABM results in enhanced differentiation of iPSCs to lung epithelia compared with Basic DM.

The decellularized lung scaffold preserves extracellular matrix proteins intact. The three-dimensional hierarchical branching structures of the airway and vasculature have recently been used to investigate regeneration of lung tissues by stem and progenitor cells. Two initial studies reported regeneration of functional lung tissues by seeding of epithelial and endothelial cells onto this decellularized lung scaffold and successful short-term functional orthotopic transplantation [36, 37]. Upon addition of mouse ESCs, the decellularized lung scaffold guided ESC differentiation toward lung-specific

lineages [12]. However, our studies demonstrated that only a limited number of undifferentiated iPSCs expressed alveolar epithelial markers during culture. This suggests that the efficiency of ESC or iPSC differentiation to lung epithelial cells by the lung scaffold is low. Jensen *et al*. seeded predifferentiated mouse ESCs into a decellularized whole lung scaffold, and then subcutaneously implanted this scaffold into mice. The implanted scaffold facilitated maintenance of lung-specific differentiation of mouse ESCs [38]. Neovascularization was confirmed in this recellularized lung scaffold after implantation.

We demonstrated the regenerative potential of differentiated iPSCs using a mouse decellularized lung scaffold model in *in vitro* three-dimensional culture. According to the results of HE staining and immunofluorescence staining, intratracheal transplantation of differentiated iPSCs into decellularized lung scaffolds resulted in formation of three-dimensional alveolar structures and differentiated alveolar epithelial cells expressing SPC or T1α protein. Differentiated iPSCs showed further maturation when cultured for 12 days in the decellularized lung scaffold.

We further investigated the therapeutic potential of differentiated iPSCs in a mouse BLM-induced lung injury model. Although only ~9% of iPSCs differentiated into SPC+ cells *in vitro*, transplantation of these unsorted differentiated iPSCs contributed to the reconstitution of BLM-injured lung and significantly reduced BLM-induced lung inflammation and fibrosis in mice. In addition to direct replacement of injured lung epithelia by differentiated iPSCs, homed iPSCs may provide beneficial effects in a paracrine manner [16, 20, 39]. Current data indicate that diverse paracrine mechanisms exist in stem cell therapy, such as modulation of cytokines, growth factors, and antimicrobial peptides [40]. In this study, we observed modulation of the inflammatory

cytokines TNF-α and IL-6 upon transplantation of differentiated iPSCs. Indeed, Yang *et al*. reported that undifferentiated iPSCs reduced endotoxin-induced acute lung injury in mice when delivered through the tail vein [41]. This effect was considered to occur in a paracrine manner and be mediated by reductions in NF-κB activity and neutrophil accumulation [41]. Transfer of MSCs also reduced BLM-induced lung injury and fibrosis partly through down-regulation of inflammatory cytokines, such as TNF-α and IL-6 [42]. However, our data showed that undifferentiated iPSCs did not sufficiently rescue the BLM-induced lung injury. This discrepancy may be due to the different degrees of acute lung injury induced by BLM and endotoxin or the different transplantation methods used.

To our knowledge, this is the first report of the three-dimensional alveolar lung structure regenerative potential and lung injury therapeutic potential of differentiated mouse iPSCs. However, because of the low efficiency of differentiation and the heterogeneity of differentiated iPSCs, the cells generated using this method are unsuitable for clinical application. A recent study reported that primordial lung progenitors can be efficiently differentiated from definitive endoderm cells through inhibition of TGFβ and BMP signaling, followed by stimulation of BMP and FGF signaling [15]. Sorting strategies can be used to enrich differentiated iPSCs. Longmire *et al*. used ESCs harboring a new Nkx2-1GFP knock-in reporter to derive primordial lung and thyroid progenitors and purified these progenitors using GFP for expansion in culture [15]. Soh *et al*. reported that lung progenitors could be enriched using the stem cell marker CD166 when differentiated from human ESCs or iPSCs [20].

CONCLUSION

We demonstrated that mouse iPSCs could acquire the alveolar epithelial cell phenotype *in vitro* under specific differentiation conditions. The differentiated iPSCs possessed the potential for regenerating three-dimensional alveolar lung structures and abrogating BLM-induced acute lung injury in the mouse.

Acknowledgments

This work was supported in part by Grants-in-Aid for Scientific Research from the Ministry of Education, Science, Sports, Culture and Technology, Japan (Nos. 22659160 and 24659396).

REFERENCES

1. Chen Z, Jin N, Narasaraju T *et al*. Identification of two novel markers for alveolar epithelial type I and II cells. Biochem Biophys Res Commun 2004;319:774–780.

2. Yamamoto K,Ferrari JD,Cao Y *et al*. Type I alveolar epithelial cells mount innate immune responses during pneumococcal pneumonia. J Immunol 2012;189:2450–2459.

3. Bishop AE. Pulmonary epithelial stem cells. Cell Proliferation 2004;37:89–96.

4. Mason RJ. Biology of alveolar type II cells. Respirology 2006;11Suppl:S12–S15.

5. Ali NN, Edgar AJ, Samadikuchaksaraei A *et al*. Derivation of type II alveolar epithelial cells from murine embryonic stem cells. Tissue Eng 2002;8:541–550.

6. Rippon HJ, Ali NN, Polak JM *et al*. Initial observations on the effect of medium composition on the differentiation of murine embryonic stem cells to alveolar type II cells. Cloning Stem Cells 2004;6:49–56.

7. Coraux C, Nawrocki-Raby B, Hinnrasky J *et al*. Embryonic stem cells generate airway epithelial tissue. Am. J. Respir. Cell Mol Biol 2005;32:87–92.

8. Samadikuchaksaraei A, Cohen S, Isaac K *et al*. Derivation of distal airway epithelium from human embryonic stem cells. Tissue Eng 2006;12:867–875.

9. Rippon HJ, Polak JM, Qin M *et al*. Derivation of distal lung epithelial progenitors from murine embryonic stem cells using a novel three-step differentiation protocol. Stem Cells 2006;24:1389–1398.

10. Roszell B, Mondrinos MJ, Seaton A *et al*. Efficient derivation of alveolar type II cells from embryonic stem cells for *in vivo* application. Tissue Eng Part A 2009;15:3351–3365.

11. Wang D, Morales JE, Calame DG *et al*. Transplantation of human embryonic stem cell-derived alveolar epithelial type II cells abrogates acute lung injury in mice. Mol Ther 2010;18:625–634.

12. Cortiella J, Niles J, Cantu A *et al*. Influence of acellular natural lung matrix on murine embryonic stem cell differentiation and tissue formation. Tissue Eng Part A 2010;16:2565–2580.

13 Lin YM, Zhang A, Rippon HJ *et al*. Tissue engineering of lung: the effect of extracellular matrix on the differentiation of embryonic stem cells to pneumocytes. Tissue Eng Part A 2010;16:1515–1526.

14. Spitalieri P, Quitadamo MC, Orlandi A *et al*. Rescue of murine silica-induced lung injury and fibrosis by human embryonic stem cells. Eur Respir J 2012;39:446–457.

15. Longmire TA, Ikonomou L, Hawkins F *et al*. Efficient derivation of purified lung and thyroid progenitors from embryonic stem cells. Cell Stem Cell 2012;10:398–411.

16. Banerjee ER, Laflamme MA, Papayannopoulou T *et al*. Human embryonic stem cells differentiated to lung lineage-specific cells ameliorate pulmonary fibrosis in a xenograft transplant mouse model. PLoS ONE 2012;7:e33165.

17. Takahashi K, Yamanaka S. Induction of pluripotent stem cells from mouse embryonic and adult fibroblast cultures by defined factors. Cell 2006;126:663–676.

18. Wernig M, Meissner A, Foreman R *et al*. *In vitro* reprogramming of fibroblasts into a pluripotent ES-cell-like state. Nature 2007;448:318–324.

19. Alipio ZA, Jones N, Liao W *et al*. Epithelial to mesenchymal transition (EMT) induced by bleomycin or TFG(b1)/EGF in murine induced pluripotent stem cell-derived alveolar Type II-like cells. Differentiation 2011;82:89–98.

20. Soh BS, Zheng D, Li Yeo JS *et al*. CD166(pos) subpopulation from differentiated human ES and iPS cells support repair of acute lung injury. Mol Ther 2012;20:2335–2346.

21. Wallis JM, Borg ZD, Daly AB *et al*. Comparative assessment of detergent-based protocols for mouse lung de-cellularization and re-cellularization. Tissue Eng Part C Methods 2012;18:420–432.

22. Jang AS, Lee JU, Choi IS *et al*. Expression of nitric oxide synthase, aquaporin 1 and aquaporin 5 in rat after bleomycin inhalation. Intensive Care Med 2004;30:489–495.

23. Lee SH, Jang AS, Kim Y *et al*. Modulation of cytokine and nitric oxide by mesenchymal stem cell transfer in lung injury/fibrosis. Respir Res 2010;8:11–16.

24. Okita K, Ichisaka T, Yamanaka S. Generation of germline-competent induced pluripotent stem cells. Nature 2007;448:313–317.

25. Daly AB, Wallis JM, Borg ZD *et al*. Initial binding and recellularization of decellularized mouse lung scaffolds with bone marrow-derived mesenchymal stromal cells. Tissue Eng Part A 2012;18:1–16.

26. Ortiz LA, Gambelli F, McBride C *et al*. Mesenchymal stem cell engraftment in lung is enhanced in response to bleomycin exposure and ameliorates its fibrotic effects. Proc Natl Acad Sci USA 2003;100:8407–8411.

27. Rojas M, Xu J, Woods CR *et al*. Bone marrow-derived mesenchymal stem cells in repair of the injured lung. Am J Respir Cell Mol Biol 2005;33:145–152.

28. Gupta N, *et al*. Intrapulmonary delivery of bone marrow-derived mesenchymal stem cells improves survival and attenuates endotoxin-induced acute lung injury in mice. J Immunol 2007;179:1855–1863.

29. Kotton DN, Fabian AJ, Mulligan RC. Failure of bone marrow to reconstitute lung epithelium. Am J Respir Cell Mol Biol 2005;33:328–334.

30. Chang JC, Summer R, Sun X *et al*. Evidence that bone marrow cells do not contribute to the alveolar epithelium. Am J Respir Cell Mol Biol 2005;33:335–342.

31. Zander DS, Baz MA, Cogle CR *et al*. Bone marrow-derived stem-cell repopulation contributes minimally to the Type II pneumocyte pool in transplanted human lungs. Transplantation 2005;80:206–212.

32. Bernard ME, Kim H, Rajagopalan MS *et al*. Repopulation of the irradiation damaged lung with bone marrow-derived cells. *In Vivo* 2012;26:9–18.

33. Samadikuchaksaraei A, Bishop AE. Effects of growth factors on the differentiation of murine ESC into type II pneumocytes. Cloning Stem Cells 2007;9:407–416.

34. Lazzaro D, Price M, de Felice M, Di Lauro R. The transcription factor TTF-1 is expressed at the onset of thyroid and lung morphogenesis and in restricted regions of the foetal brain. Development 1991;113:1093–1104.

35. Maeda Y, Davé V, Whitsett JA. Transcriptional control of lung morphogenesis. Physiol Rev 2007;87:219–44.

36. Petersen TH, Calle EA, Zhao L *et al*. Tissue-engineered lungs for *in vivo* implantation. Science 2010;329(5991):538–541.

37. Ott HC, Clippinger B, Conrad C *et al*. Regeneration and orthotopic transplantation of a bioartificial lung. Nature Medicine 2010;16:927–933.

38. Jensen T, Roszell B, Zang F *et al*. A rapid lung de-cellularization protocol supports embryonic stem cell differentiation *in vitro* and following implantation. Tissue Eng Part C Methods 2012;18:632–646.

39. Gnecchi M, Zhang Z, Ni A, Dzau VJ. Paracrine mechanisms in adult stem cell signaling and therapy. Circ Res 2008;103:1204–1219.

40. Maron-Gutierrez T, Laffey JG, Pelosi P, Rocco PR. Cell-based therapies for the acute respiratory distress syndrome. Curr Opin Crit Care 2013; Dec 2. [Epub ahead of print]

41. Yang KY, Shih HC, How CK et al. IV delivery of induced pluripotent stem cells attenuates endotoxin-induced acute lung injury in mice. Chest 2011;140:1243–1253.

42. Lee SH, Jang AS, Kim YE, Cha JY, Kim TH, Jung S. et al. Modulation of cytokine and nitric oxide by mesenchymal stem cell transfer in lung injury/fibrosis. Respir Res 2010;11:16.

FIGURE LEGENDS

Figure 1. Differentiation media based on mRNA expression levels of endodermal and lung epithelial markers A: Differentiation protocols for the derivation of alveolar epithelial cells from mouse iPSCs using a dissociated seeding method. B: Quantitative polymerase chain reaction analysis of lung epithelial markers on day 12. *P<0.05 versus D12-①; # P<0.01 versus D12-②; ▲P<0.01 versus D12-①.

C: Quantitative polymerase chain reaction (qPCR) analysis of lung epithelial markers in differentiated iPSCs D12-② compared with the murine type II pneumocyte cell line MLE12 and mouse lung tissue. Expression ratios were normalized to the GAPDH expression level. Data are representative of three independent experiments. Note that the y-axis is a logarithmic scale.

Figure 2. Evaluation of differentiated iPSC phenotypes on Day 12

A: iPS cells differentiated for 12 days were immunostained with goat anti-mouse pro-SPC antibody (red) or goat IgG and nuclear-counterstained with DAPI (blue). Scale bars: 50 μm. B: Flow cytometry analysis of SPC expression. C: Transmission electron micrographs of MLE12 cells (a murine type 2 pneumocyte cell line) and differentiated iPSCs. Upper-left: MLE12 cells exhibit characteristic lamellar bodies (black arrows) and apical microvilli (red arrows). Upper-right: Magnified view of the upper-left image. Lower-left: Mouse differentiated iPSCs showing similar lamellar bodies and microvilli to those of MLE12 cells. Lower-right: Magnified view of the lower-left image. Scale bars: 1 μm.

Figure 3. Decellularization and recellularization of mouse lung

A: A photo and schematic illustration of decellularization and recellularization **B:** HE staining of sections of a decellularized mouse lung scaffold (no cell) and recellularized lung tissues reseeded with fibroblasts, undifferentiated iPSCs, or differentiated iPSCs on D12. Bottom panels show magnified views of the dotted line areas in upper panels. Scale bar: 100 μm for upper panels, 50 μm for bottom panels.

Figure 4. Immunofluorescence staining of the alveolar type-II cell marker SPC and alveolar type-I cell marker T1α in recellularized lung tissues. Decellularized lung scaffolds were reseeded with mouse fibroblasts, undifferentiated iPSCs, or differentiated iPSCs and immunostained with goat anti-mouse pro-SPC or T1α antibodies after 12 days. Yellow arrows indicate SPC^+ or $T1\alpha^+$ cells. Bottom panels show magnified views of the areas marked by the dotted lines in the upper panels. Scale bar: 50 μm for upper panels, 10 μm for lower panels.

Figure 5. Immunofluorescence staining of the alveolar type-II cell marker SPC in mouse lung tissues

Following intratracheal exposure to normal saline or 4 U/kg bleomycin (BLM), fibroblasts, undifferentiated iPSCs, or differentiated iPSCs labeled with PKH26 cell tracker (red) were instilled intratracheally into mice on day 2. The lung tissues were excised on day 12 and immunostained with goat anti-mouse pro-SPC antibody (green). Nuclei were counterstained with DAPI (blue). Yellow arrows indicate $PKH26^{+}/SPC^{+}$ cells. Scale bars: 50 μm. A magnified view of a $PKH26^{+}/SPC^{+}$ cell is indicated by dotted lines. Bottom panels show magnified views of the areas marked by the dotted lines in the upper panels. Scale bar: 50 μm for upper panels, 10 μm for lower panels.

Figure 6. Amelioration of lung fibrosis by transplantation of iPSCs-derived AECs in BLM-treated mice

Following intratracheal exposure of normal saline or 4 U/kg BLM, fibroblasts, undifferentiated iPSCs, or differentiated iPSCs were instilled intratracheally into mice on day 2. The lung tissues were excised on day 12. A: HE and Sirius red/Fast green staining of lung sections. Scale bar: 100 μm. Magnified views of the white dotted line areas were marked with yellow dotted lines. B: The wet/dry ratio of lungs on day 12. Data are expressed as the mean±SD; n= ≥7/group; * * $P<0.01$ *versus* the saline control group; ▲$P>0.05$ *versus* the BLM group; *$P<0.05$ *versus* the saline control group; # $P<0.01$ *versus* the BLM and BLM/fibroblasts groups. C: Collagen deposition in lung tissue was evaluated qualitatively by hydroxyproline assay. Data are expressed as the mean±SD; n= ≥5/group; * * $P<0.01$ *versus* the saline control group; ▲$P>0.05$ *versus*

the BLM group; *P<0.05 *versus* the saline control group; # P<0.01 *versus* the BLM and BLM/fibroblasts groups.

Figure 7. Effect of differentiated iPSC transplantation on the BALF profile in BLM-treated mice

Following intratracheal exposure to normal saline or 4 U/kg BLM, fibroblasts, undifferentiated iPSCs, or differentiated iPSCs were instilled intratracheally into mice on day 2. BAL was performed on day 12. A: BAL fluids from the four groups were cytospinned, and the cell pallets were stained using Diff-Quik. Representative images are shown. Yellow arrows indicate neutrophils and black arrows lymphocytes. Scale bar: 50 μm. IL-6 (B) and TNF-α (C) concentrations in BAL fluids were measured using sandwich ELISA kits. Data are expressed as the means ± SD; n ≥ 5 per group; B: * P<0.05 versus the saline control group; ▲ P>0.05 versus the BLM group and BLM/fibroblasts group; # P<0.05 versus the BLM group; † P>0.05 versus the saline control group; C: ** P<0.01 versus the saline control group; * P<0.05 versus the saline control group; ▲ P>0.05 versus the BLM group and BLM/fibroblasts group; # P<0.01 versus the BLM group; P<0.05 versus the BLM/fibroblasts group; †P>0.05 versus the saline control group.

Figure S1. The pluripotency of undifferentiated iPS cells (D0) at passage 30

A: Immunofluorescence staining of mouse iPSCs with the stem cell markers OCT4 and SSEA1. The GFP gene was knocked-in under the Nanog promoter, allowing detection of GFP (green) in undifferentiated cells. Scale bar: 200 μm for upper panels, 100 μm for bottom panels. B: Alkaline phosphatase staining. Bottom panel show magnified view of

the area marked by the dotted lines in the upper panel. Scale bar: 100 μm for upper panel, 50 μm for bottom panel. C: Flow cytometry analysis of mouse iPS cells using SSEA1 and OCT4.

Figure S2. Expression of the endoderm markers Sox17 and Foxa2 in iPSCs on day 7 of differentiation

A: iPS cells differentiated for 6 days were immunostained using goat anti-mouse Sox17 and Foxa2 antibodies (red) and were nuclear-counterstained with DAPI (blue). Scale bar: 50 μm. B: qRT-PCR analysis of Sox17 and Foxa2 on day 7 of differentiation. **P*<0.05 *versus* Basic DM

.

Figure S3. Immunofluorescence staining of the alveolar type-I cell marker T1α in mouse lung tissues

Following intratracheal exposure to normal saline or 4 U/kg BLM, fibroblasts, undifferentiated iPSCs, or differentiated iPSCs labeled with PKH26 cell tracker (red) were instilled intratracheally into mice on day 2. The lung tissues were excised on day 12 and immunostained with a goat anti-mouse T1α antibody (membrane staining, green). Nuclei were counterstained with DAPI (blue). Yellow arrows indicate $PKH26^{+}/T1\alpha^{+}$ cells. Scale bars: 50 μm. A magnified view of a $PKH26^{+}/T1\alpha^{+}$ cell is indicated by dotted lines. Bottom panels show magnified views of the areas marked by the dotted lines in the upper panels. Scale bar: 50 μm for upper panels, 10 μm for lower panels.

Figure S4. Recovery of SPC+ cells and identification of transplanted differentiated iPSCs in the BLM-injured lung

A: Quantification of SPC+ cells in lung tissues after differentiated iPSC transplantation in the BLM-injured lung on day 12. ** $P<0.01$ versus the saline control group; * $P<0.05$ versus the saline control group; †$P>0.05$ versus the BLM group; # $P<0.05$ versus the BLM group; ▲ $P>0.05$ versus the saline control group. B: SPC and T1α immunofluorescence in lung tissues transplanted with PKH26-stained differentiated iPSCs after BLM challenge on day 30. Yellow arrows indicate PKH26+/SPC+ or PKH26+/T1α+ cells. Scale bar: 30 μm

Figure 1

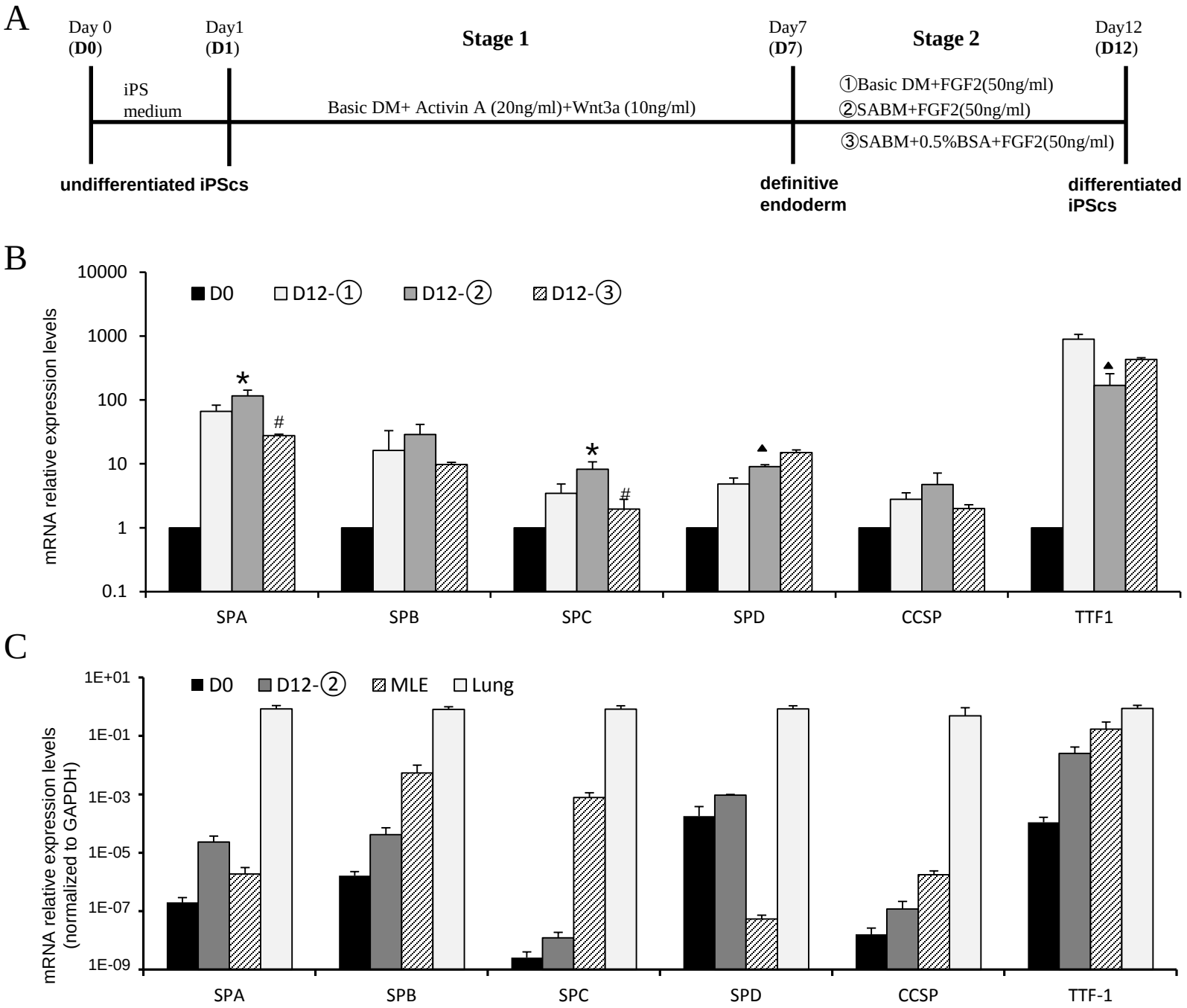
A
Day 0
(D0)
Day1
(D1)
Stage 1
Day7
(D7)
Stage 2
Day12
(D12)
iPS
medium
Basic DM+ Activin A (20ng/ml)+Wnt3a (10ng/ml)
①Basic DM+FGF2(50ng/ml)
②SABM+FGF2(50ng/ml)
③SABM+0.5%BSA+FGF2(50ng/ml)
undifferentiated iPScs
definitive
endoderm
differentiated
iPScs
B
mRNA relative expression levels
D0
D12-①
D12-②
D12-③
10000
1000
100
10
1
0.1
SPA
SPB
SPC
SPD
CCSP
TTF1
C
mRNA relative expression levels
(normalized to GAPDH)
D0
D12-②
MLE
Lung
1E+01
1E-01
1E-03
1E-05
1E-07
1E-09
SPA
SPB
SPC
SPD
CCSP
TTF-1

Figure 2

A

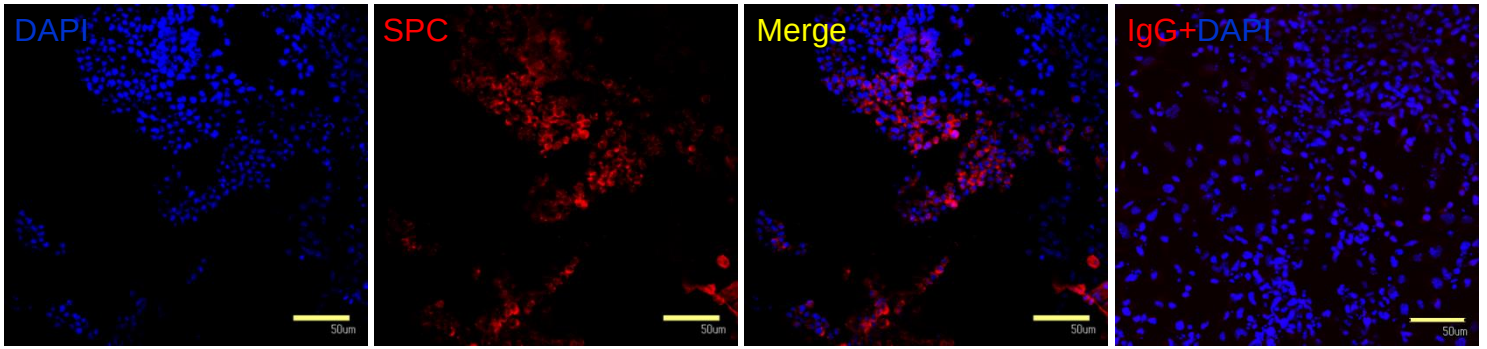
DAPI
SPC
Merge
IgG+DAPI
50um

B

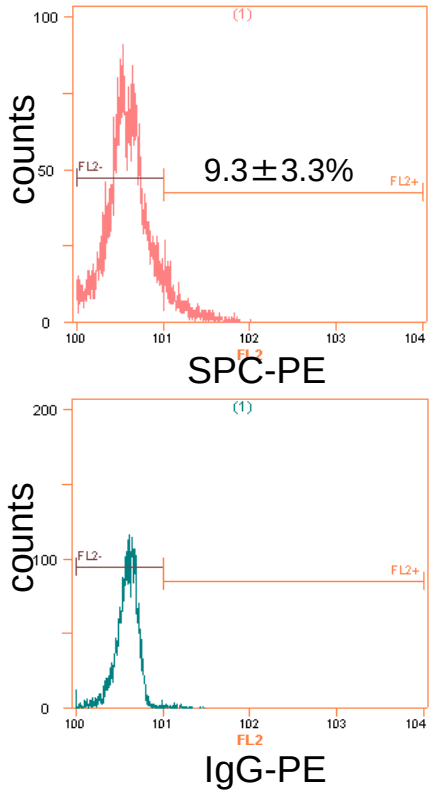
counts
9.3±3.3%
FL2-
FL2+
SPC-PE
IgG-PE
FL2

C

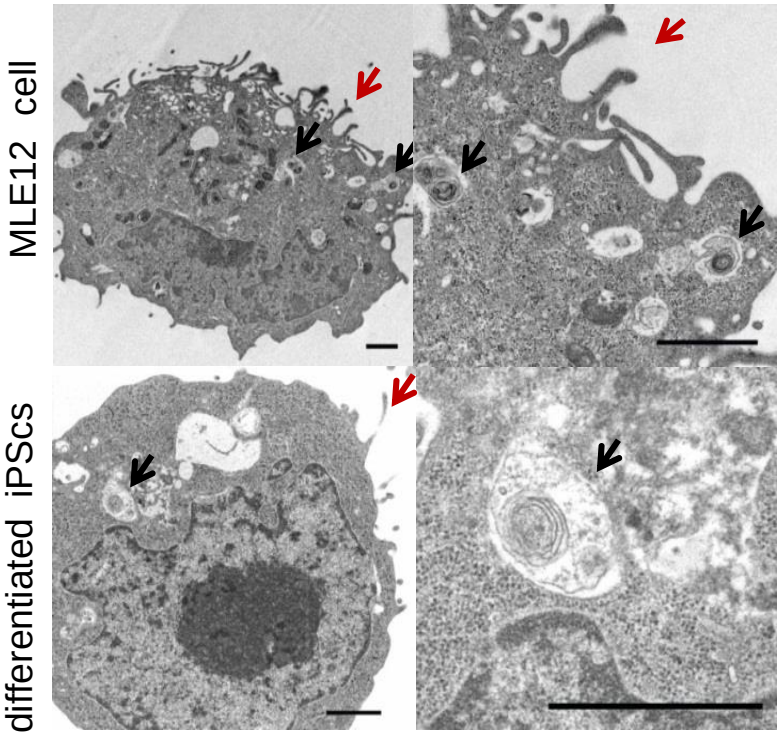
MLE12 cell
differentiated iPScs

Figure 3

A

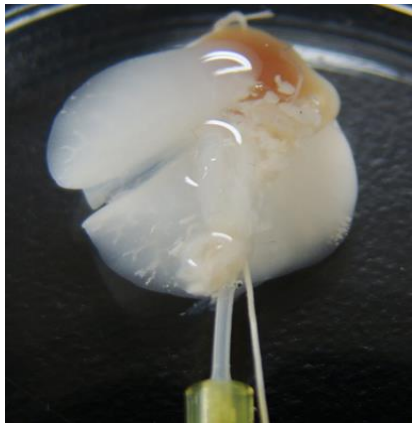

decellurarized lung

2×10^6 cells/mouse

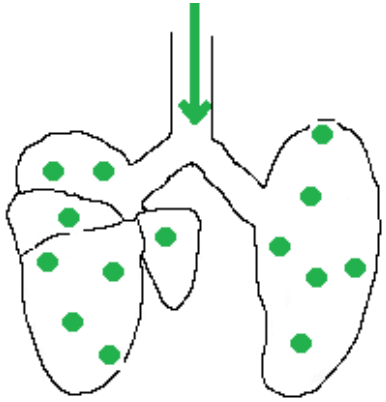

recellurarization of lung

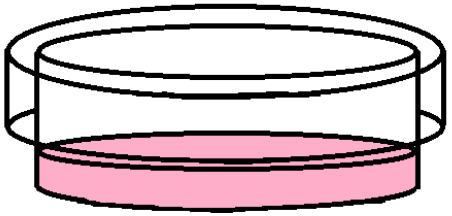

Lung slices were cultured in Small Airway Epithelial Cell Growth Medium (SAGM) for 12days

B

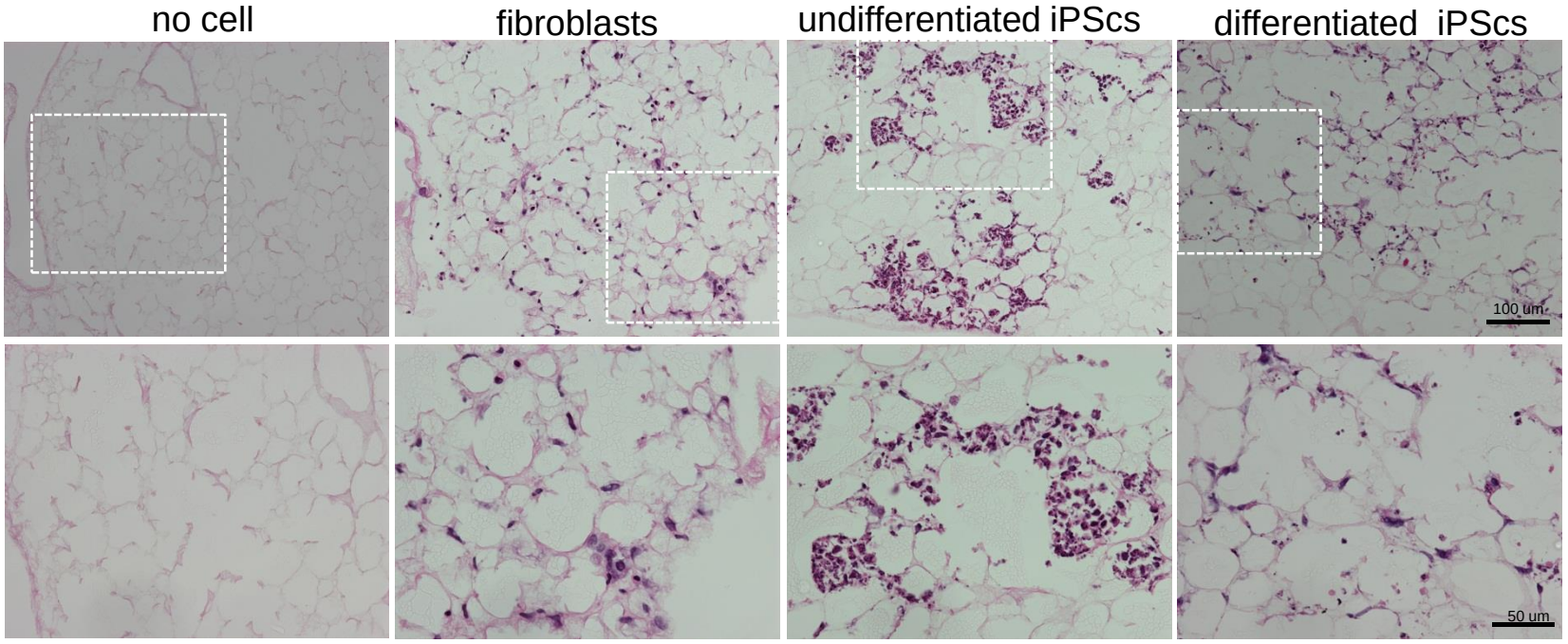

Figure 4

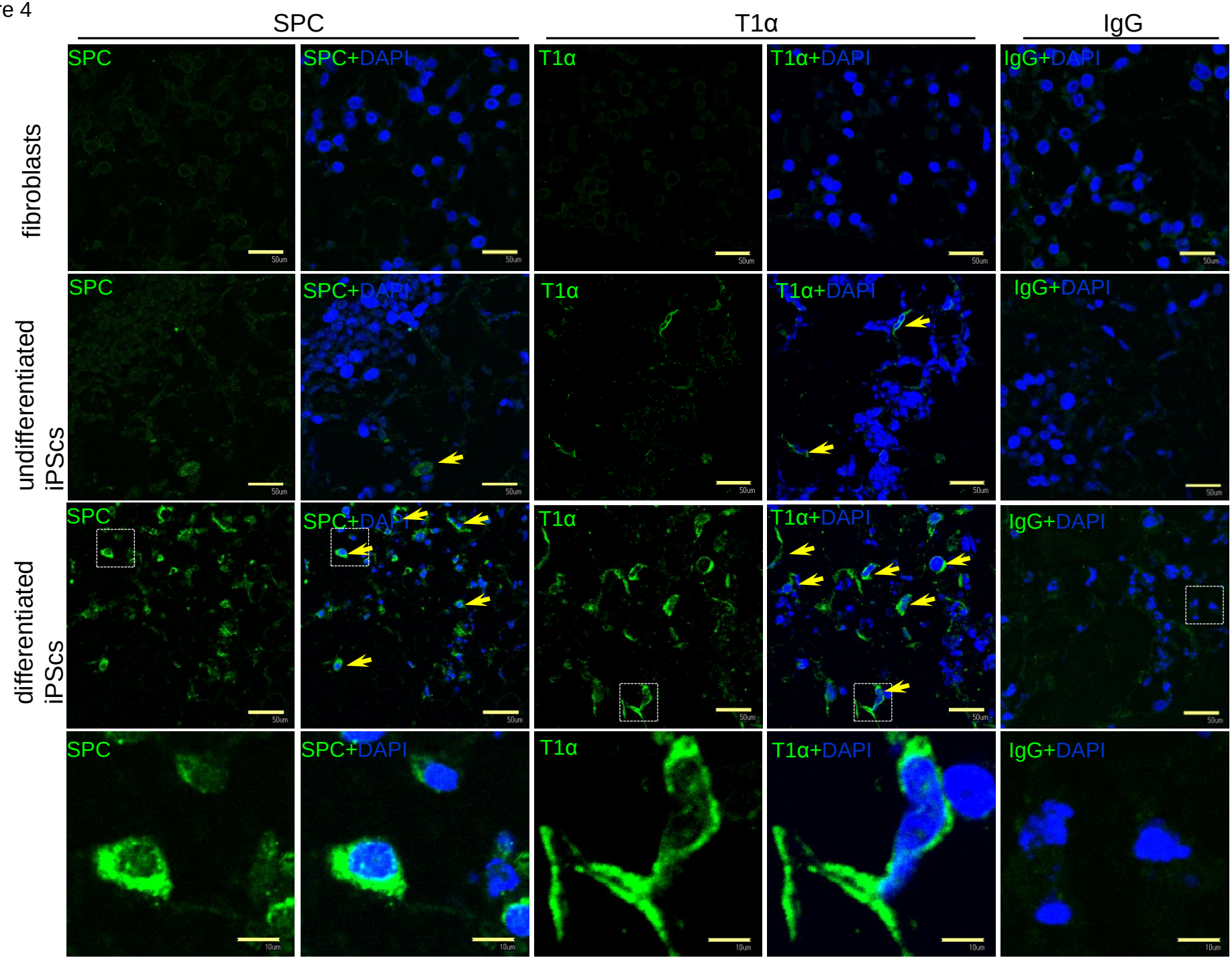
SPC
T1α
IgG
fibroblasts
undifferentiated iPScs
differentiated iPScs
SPC
SPC+DAPI
T1α
T1α+DAPI
IgG+DAPI
50um
10um

Figure 5

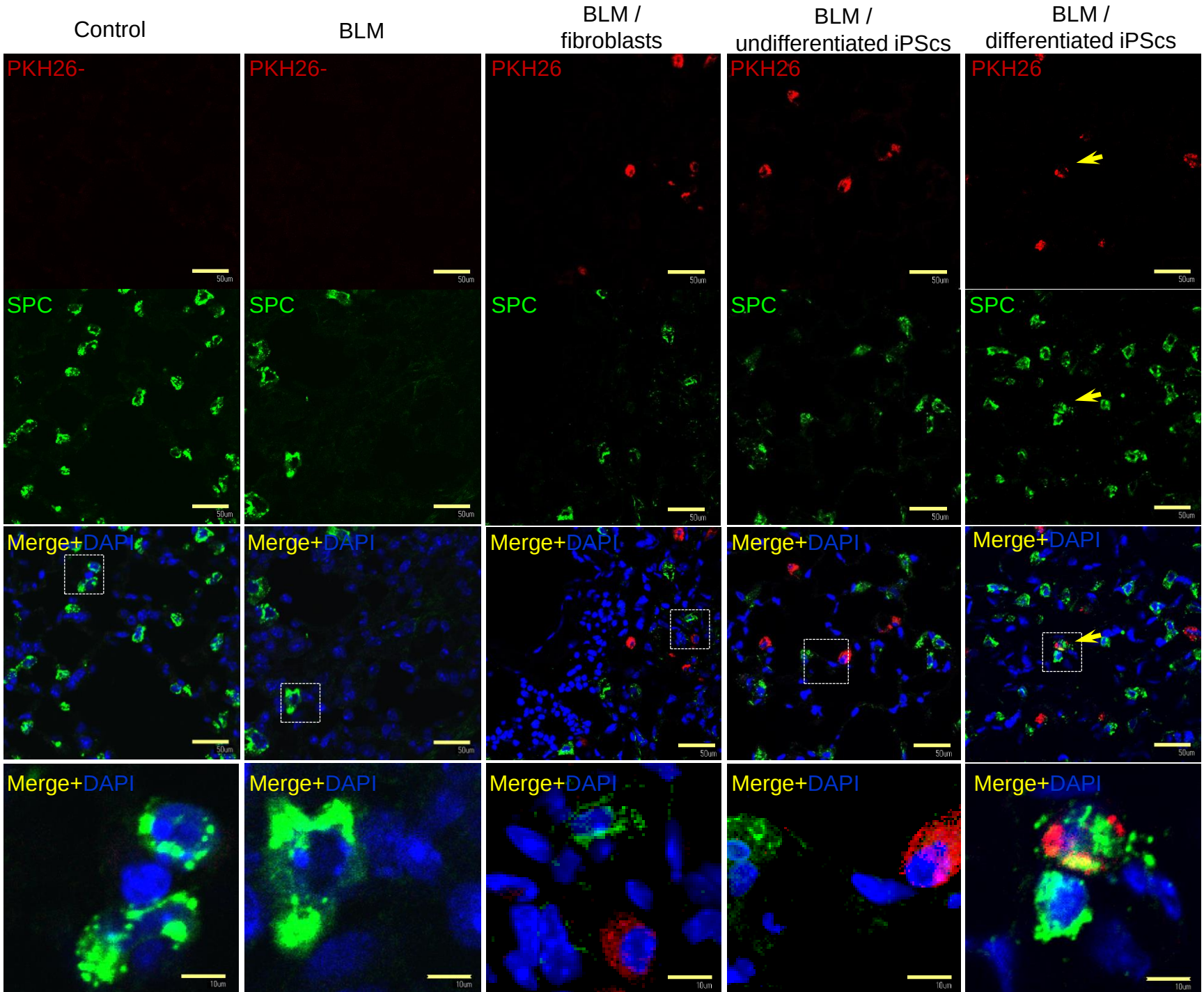
Control
BLM
BLM / fibroblasts
BLM / undifferentiated iPScs
BLM / differentiated iPScs
PKH26-
PKH26-
PKH26
PKH26
PKH26
SPC
SPC
SPC
SPC
SPC
Merge+DAPI
Merge+DAPI
Merge+DAPI
Merge+DAPI
Merge+DAPI
Merge+DAPI
Merge+DAPI
Merge+DAPI
Merge+DAPI
Merge+DAPI
50um
10um

Figure 6

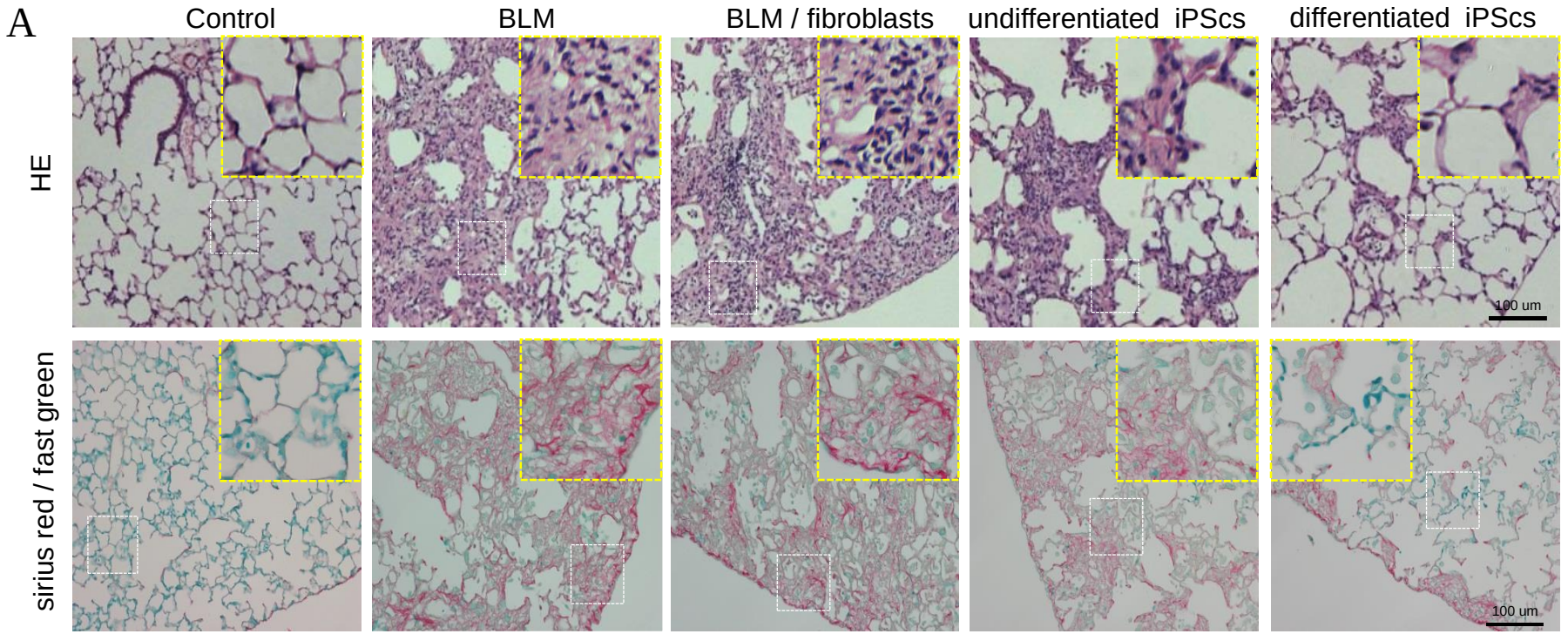
A
Control
BLM
BLM / fibroblasts
BLM / undifferentiated iPScs
BLM / differentiated iPScs
HE
sirius red / fast green
100 um
100 um

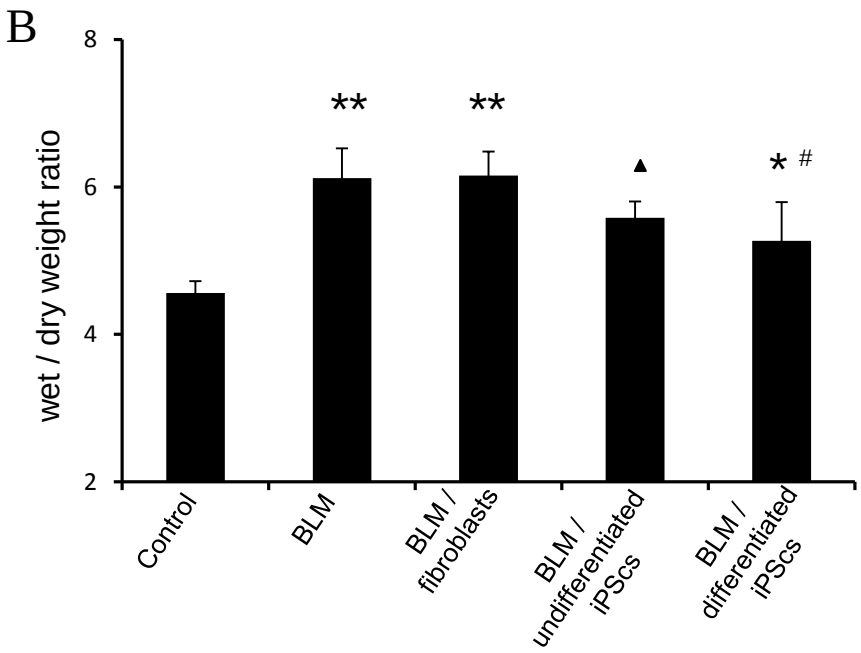
B
wet / dry weight ratio
8
6
4
2
**
**
▲
* #
Control
BLM
BLM / fibroblasts
BLM / undifferentiated iPScs
BLM / differentiated iPScs

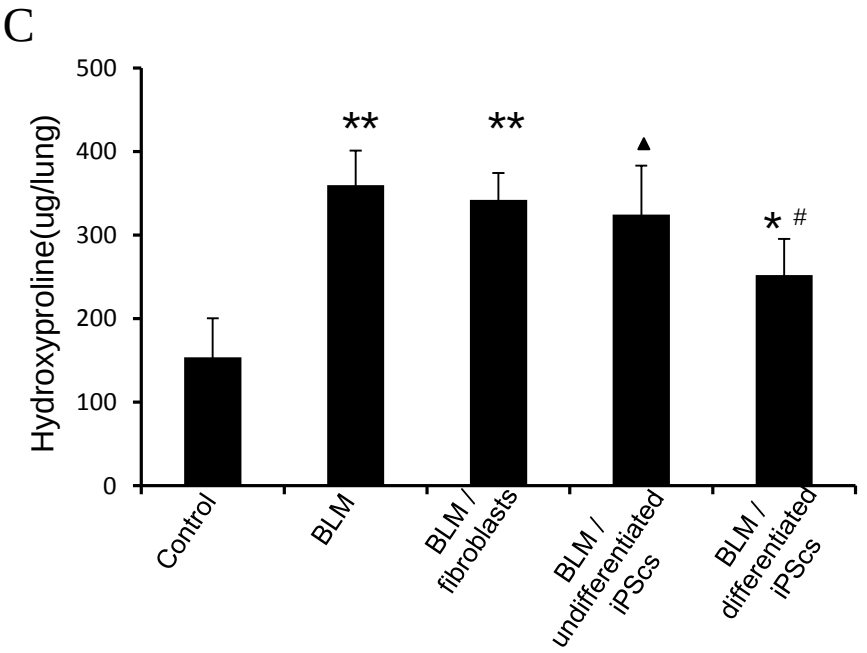
C
Hydroxyproline(ug/lung)
500
400
300
200
100
0
**
**
▲
* #
Control
BLM
BLM / fibroblasts
BLM / undifferentiated iPScs
BLM / differentiated iPScs

Figure 7

A

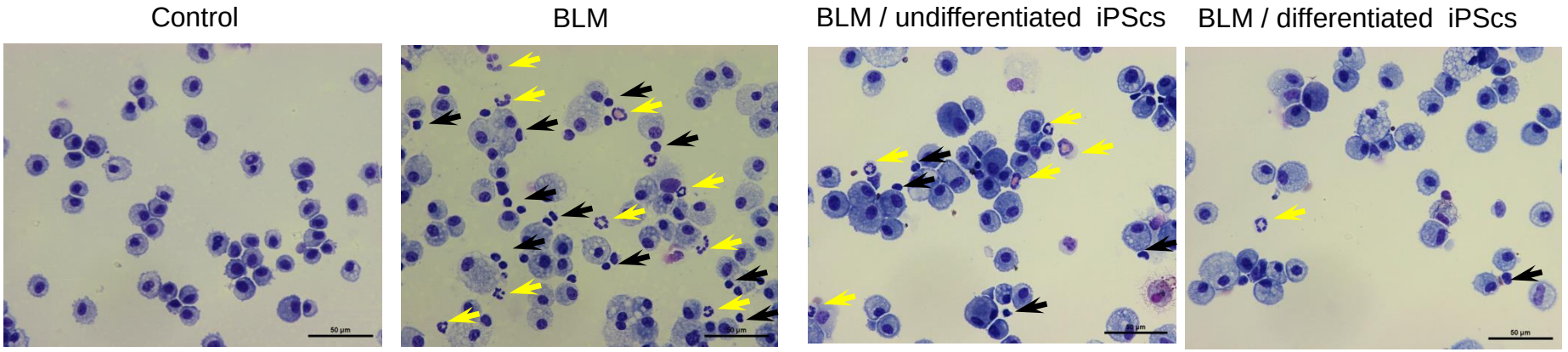
Control
BLM
BLM / undifferentiated iPScs
BLM / differentiated iPScs

B

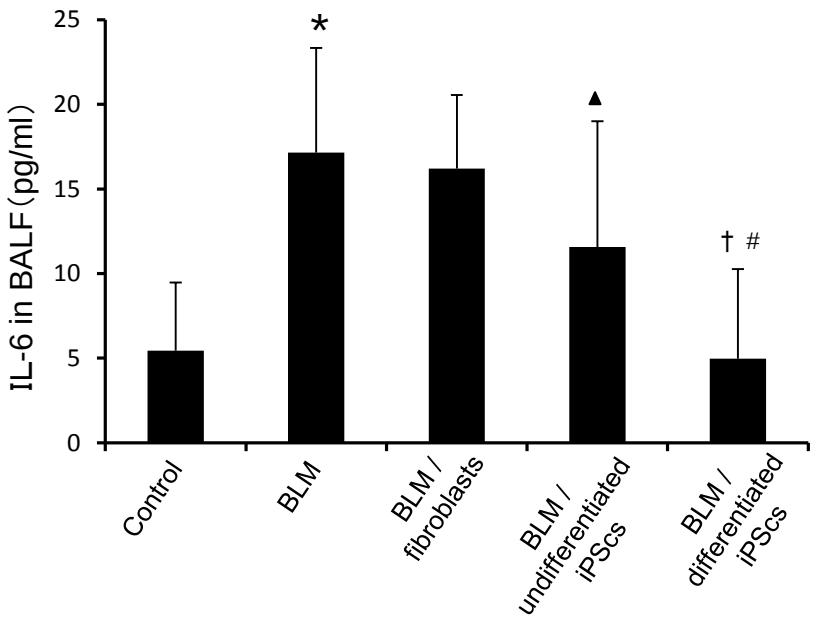
IL-6 in BALF (pg/ml)
25
20
15
10
5
0
*
† #
Control
BLM
BLM / fibroblasts
BLM / undifferentiated iPScs
BLM / differentiated iPScs

C

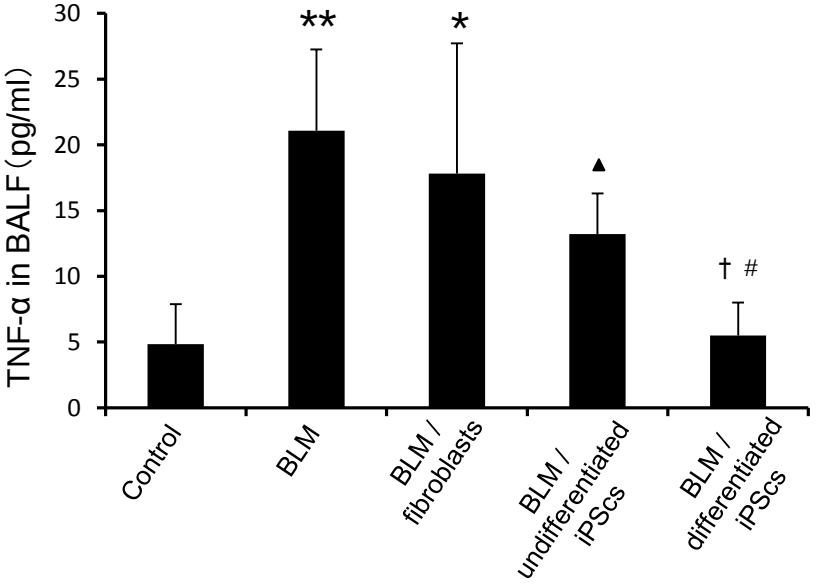
TNF-α in BALF (pg/ml)
30
25
20
15
10
5
0
**
*
† #
Control
BLM
BLM / fibroblasts
BLM / undifferentiated iPScs
BLM / differentiated iPScs

Figure S1

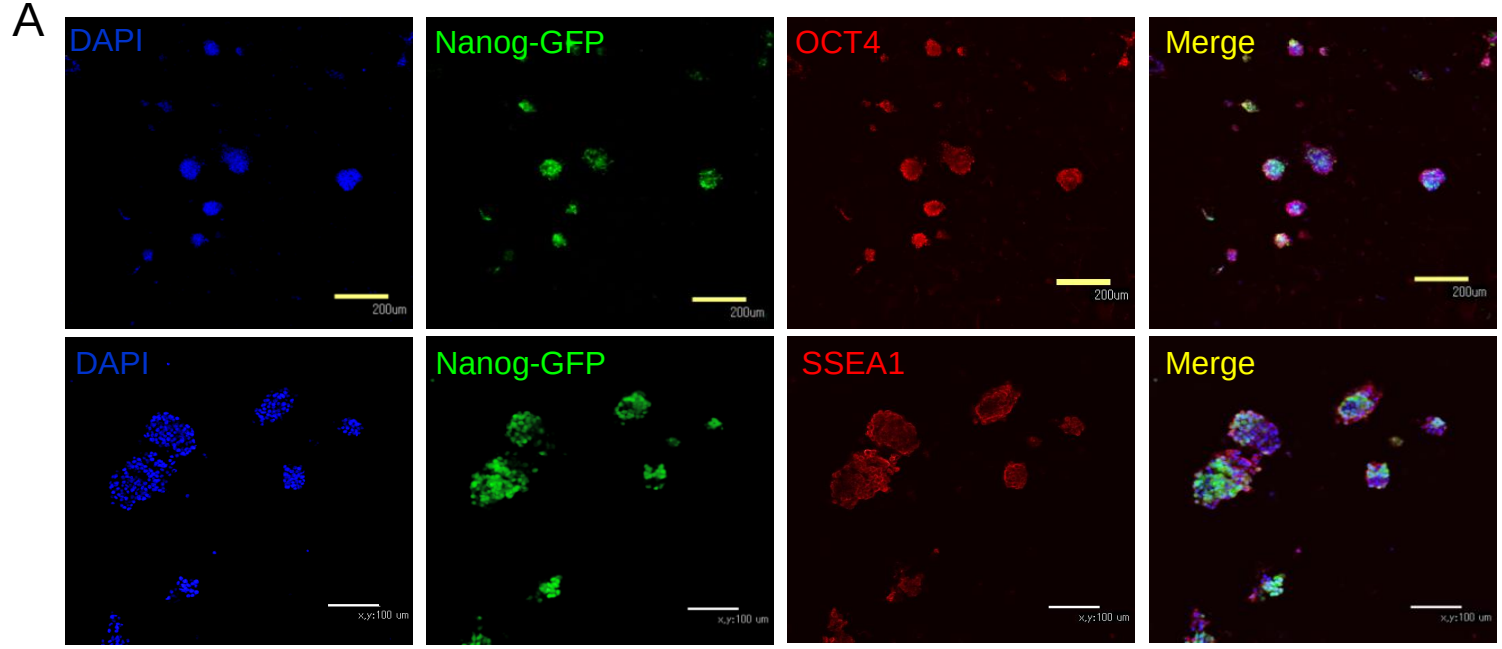
A
DAPI
Nanog-GFP
OCT4
Merge
DAPI
Nanog-GFP
SSEA1
Merge
200um
x,y:100 um
B
100 um
50 um
C
counts
0.13%
91.3%
IgG
SSEA1-PE
0.96%
82.4%
IgG
OCT4-PE
FL2-
FL2+
FL2

Figure S2

A

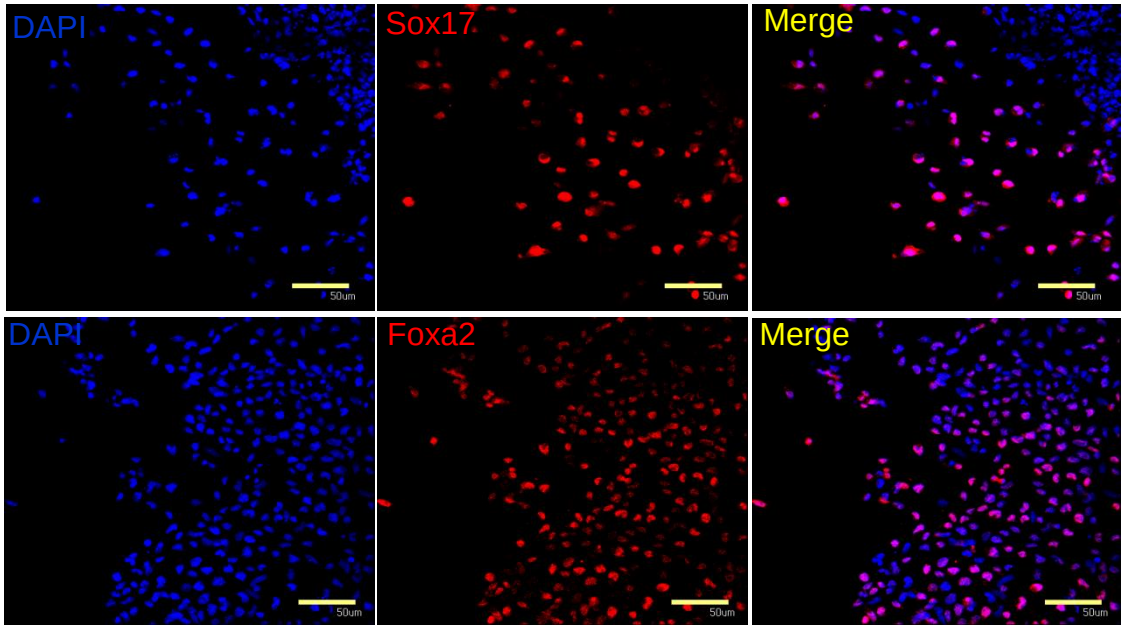
DAPI
Sox17
Merge
DAPI
Foxa2
Merge
50um

B

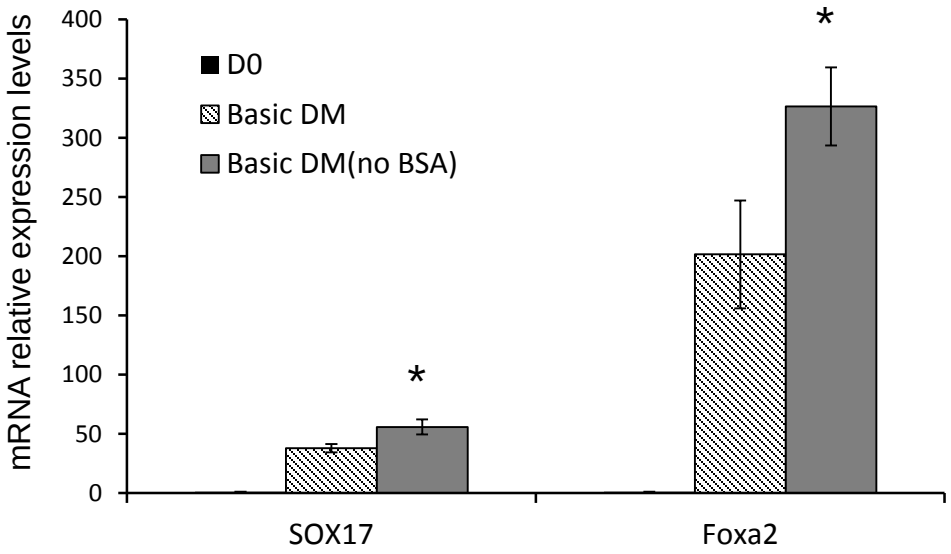
mRNA relative expression levels
400
350
300
250
200
150
100
50
0
D0
Basic DM
Basic DM(no BSA)
*
*
SOX17
Foxa2

Figure S3

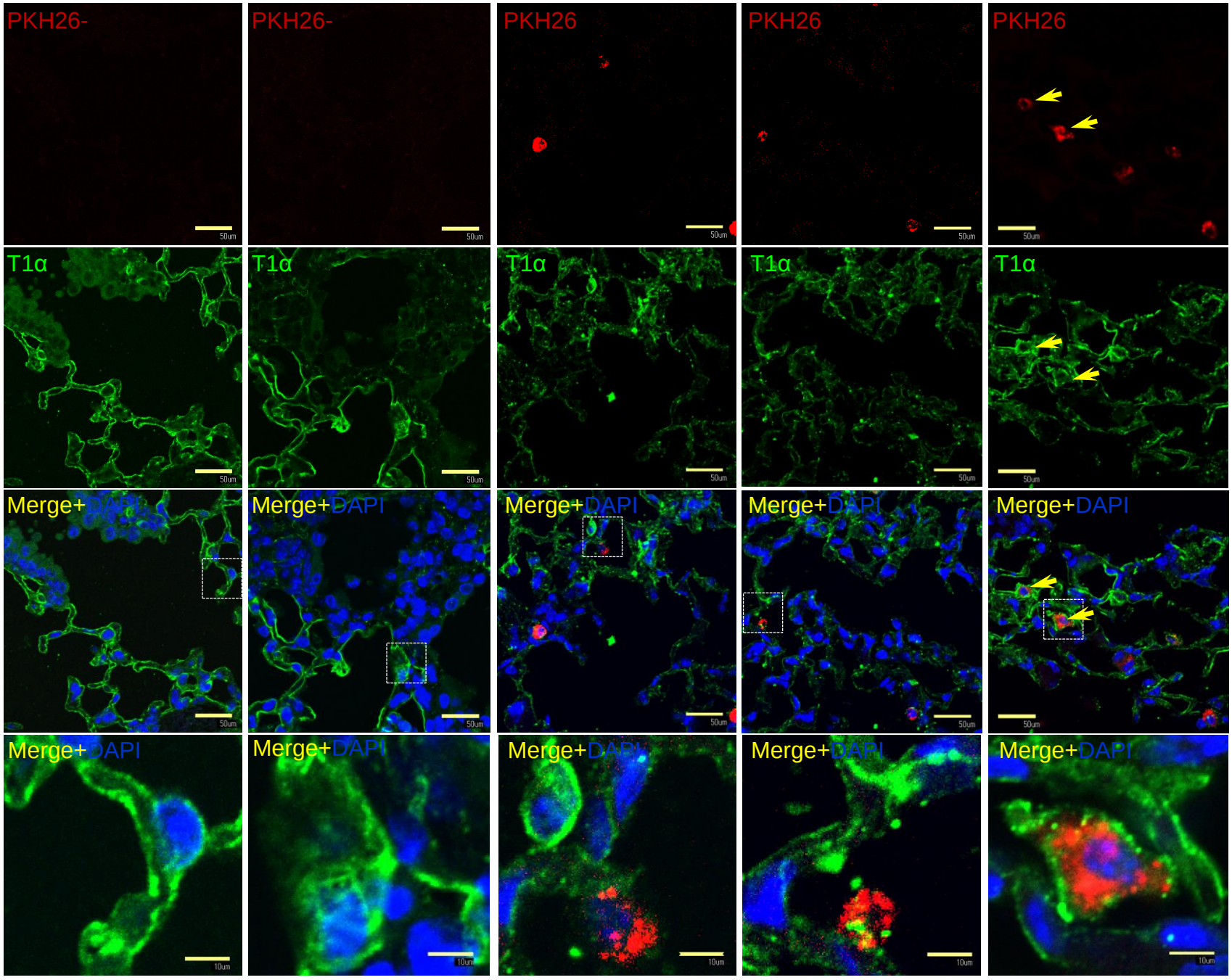
Control
BLM
BLM / fibroblasts
BLM / undifferentiated iPScs
BLM / differentiated iPScs
PKH26-
PKH26-
PKH26
PKH26
PKH26
T1α
T1α
T1α
T1α
T1α
Merge+DAPI
Merge+DAPI
Merge+DAPI
Merge+DAPI
Merge+DAPI
Merge+DAPI
Merge+DAPI
Merge+DAPI
Merge+DAPI
Merge+DAPI
50um
10um

Figure S4

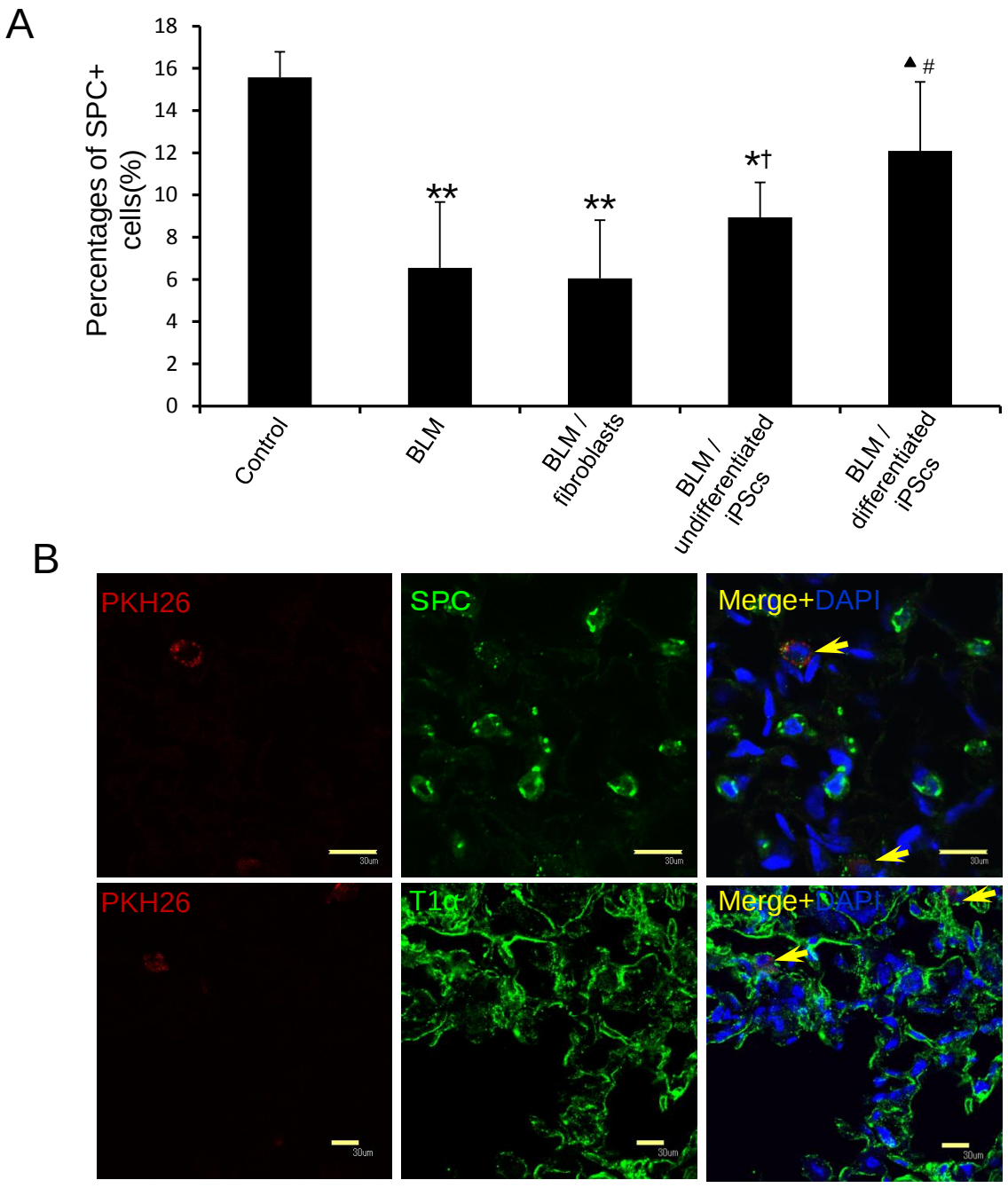
A
Percentages of SPC+ cells(%)
18
16
14
12
10
8
6
4
2
0
**
**
*†
▲#
Control
BLM
BLM / fibroblasts
BLM / undifferentiated iPScs
BLM / differentiated iPScs
B
PKH26
SPC
Merge+DAPI
PKH26
T1α
Merge+DAPI
30um